Title: Directed evolution of the rRNA methylating enzyme Cfr reveals molecular basis of antibiotic resistance

Short Title: Directed evolution of Cfr resistance enzyme

Authors: Kaitlyn Tsai[1], Vanja Stojković[1], Lianet Noda-Garcia[2], Iris D. Young[3], Alexander G. Myasnikov[4], Jordan Kleinman[1], Ali Palla[1], Stephen N. Floor[5,6], Adam Frost[4,7], James S. Fraser[3,7], Dan S. Tawfik[2], Danica Galonić Fujimori[1,7,8]*

Affiliations:

[1]Department of Cellular and Molecular Pharmacology; University of California San Francisco; San Francisco, CA 94158, USA.

[2]Department of Biomolecular Sciences, Weizmann Institute of Science; Rehovot, Israel.

[3]Department of Bioengineering and Therapeutic Sciences, University of California San Francisco; San Francisco, CA 94158, USA.

[4]Department of Biochemistry and Biophysics, University of California San Francisco; San Francisco, CA 94158, USA.

[5]Department of Cell and Tissue Biology, University of California San Francisco; San Francisco, CA 94143, USA.

[6]Helen Diller Family Comprehensive Cancer Center, University of California San Francisco; San Francisco, CA 94143, USA.

[7]Quantitative Biosciences Institute, University of California San Francisco; San Francisco, CA 94158, USA.

[8]Department of Pharmaceutical Chemistry, University of California San Francisco; San Francisco, CA 94158, USA.

*Corresponding author. Email: Danica.Fujimori@ucsf.edu

Abstract:

Many clinically useful antibiotics inhibit the bacterial ribosome. The ribosomal RNA-modifying enzyme Cfr methylates an adenosine (m^8A2503) in the peptidyl transferase center and causes cross-resistance to several classes of antibiotics. Despite the prevalence of this mode of resistance, mechanisms of adaptation to antibiotic pressure that exploit ribosome modification by Cfr are poorly understood. Moreover, direct evidence for how m^8A2503 alters antibiotic binding sites within the ribosome is lacking. To address these questions, we evolved Cfr under antibiotic selection to generate variants that confer increased resistance and methylation of rRNA, provided by enhanced Cfr expression and stability. Using a variant which achieves near-stoichiometric methylation, we determined a 2.2Å cryo-EM structure of the Cfr-modified ribosome, revealing the molecular basis for resistance and informing design of antibiotics that overcome Cfr resistance.

One Sentence Summary:

Directed evolution of Cfr identifies adaptive strategies and enables structural determination of an antibiotic-resistant ribosome.

Key words:

Cfr; directed evolution; antibiotic resistance; RNA modification; A2503; 23S rRNA; peptidyl transferase center; cryo-EM structure

Main Text:

A large portion of clinically-relevant antibiotics halt bacterial growth by binding to the ribosome and inhibiting protein synthesis (*1–3*). Since antibiotic binding sites are primarily composed of ribosomal RNA (rRNA), rRNA-modifying enzymes that alter antibiotic binding pockets are central to evolved resistance (*4*, *5*). The rRNA-methylating enzyme Cfr modifies an adenosine nucleotide located within the peptidyl transferase center (PTC), a region of the ribosome essential for catalyzing peptide bond formation and consequently, a common target for antibiotics (*6*, *7*). Cfr is a radical SAM enzyme that methylates the C8 carbon of adenosine at position 2503 (m^8A2503, *E. coli* numbering) (*8–12*). Due to the proximal location of A2503 to many antibiotic binding sites, introduction of a single methyl group is sufficient to cause resistance to eight classes of antibiotics simultaneously: **ph**enicols, **l**incosamides, **o**xazolidinones, **p**leuromutilins, **s**treptogramin **A** ($PhLOPS_A$), in addition to nucleoside analog A201A, hygromycin A, and 16-membered macrolides (*13–15*). Among rRNA modifying enzymes, this extensive cross-resistance phenotype is unique to Cfr and highly problematic clinically.

Cfr emergence in human pathogens appears to be a recent event, with the first case reported in 2007 from a patient-derived *Staphylococcus aureus* isolate (*16*, *17*). Since then, the *cfr* gene has been identified across the globe in both gram-positive and gram-negative bacteria (*18*, *19*), and has been associated with several clinical resistance outbreaks to the oxazolidinone antibiotic, linezolid (*20–27*). The vast spread of Cfr is largely attributed to its association with mobile genetic elements and relatively low impact on bacterial fitness, suggesting that *cfr* can be rapidly disseminated within bacterial populations and to pathogens (*28*, *29*).

Due to its alarming cross-resistance phenotype, it is critical to understand how bacteria may adapt under antibiotic pressure to enhance Cfr activity and bolster protection against ribosome antibiotics. Identification of Cfr mutations that improve resistance will also be critical for informing clinical surveillance and designing strategies to counteract resistance. A major limitation of the current understanding on Cfr-mediated resistance is the lack of structural insight into changes in the ribosome that result from Cfr modification. Steric occlusion of antibiotic binding has been proposed as a model to rationalize altered antibiotic susceptibility (*15*). Additionally, the observation that A2503 can adopt both *syn* and *anti*-conformations in previously reported ribosome structures suggests the possibility that methylation may regulate conformation of the base, as previously proposed (*30–33*). However, direct evidence for how m^8A2053 alters antibiotic binding sites within the ribosome PTC is lacking.

In this study, we sought to identify mechanisms that can enhance antibiotic resistance through directed evolution, under antibiotic selection, of a *cfr* found in a clinical MRSA isolate (*34*). The obtained highly resistant Cfr variants show increased rRNA methylation, driven primarily by robust improvements in Cfr cellular levels, achieved either by higher transcription or increased translation and improved cellular stability. In particular, mutation of the second Cfr amino acid to lysine strongly enhances translation and resistance. Lastly, we used an evolved variant which achieves near-stoichiometric rRNA methylation to generate a high-resolution cryo-EM structure of the Cfr-modified *E. coli* ribosome. The obtained structural insights provide a rationale for how m^8A2503 causes resistance to ribosome antibiotics.

Results

Evolved Cfr variants confer enhanced antibiotic resistance

To perform directed evolution of Cfr, we used error-prone PCR (EP-PCR) to randomly introduce 1-3 mutations into the *cfr* gene obtained from a clinical MRSA isolate (*16*) (Fig. 1A). Mutagenized *cfr* sequences were then cloned into a pZA vector where Cfr was expressed under tetracycline-inducible promoter P_{tet} introduced to enable precise control of Cfr expression (*35*). The resulting library of ~10^7 *E. coli* transformants was selected for growth in the presence of increasing amounts of tiamulin, a pleuromutilin antibiotic to which Cfr confers resistance. During each round, a small subset of the surviving colonies were sequenced to identify new mutations. After two rounds of evolution, *wild-type* Cfr was no longer detected, indicating that the introduced mutations provide enhanced survivability in the presence of tiamulin. After five rounds of mutation and selection, we performed two rounds of selection without mutagenesis, and with high tiamulin concentrations, thus leading to fixation of mutations that provide robust resistance.

Analysis of surviving *cfr* sequences from the final rounds of selection revealed notable trends (table S2). Three positions were primarily mutated: N2, I26, and S39. By homology modeling, these mutational hotspots appear distal from the enzyme active site (>12 Å; Fig. 1B). Second, ~28% of sequences contained alterations to the promoter. These alterations consist of either P_{tet} duplication, or insertion of a partial P_{tet} sequence (table S3). And third, all selected variants contained a premature stop codon that results in the loss of the C-terminal His_6-tag, suggesting that its presence hampers the ability of Cfr to confer robust resistance. Thus, in all subsequent experiments, the cellular activity of evolved variants was compared to *wild-type* Cfr lacking a C-terminal His_6-tag, herein referred to CfrWT.

We selected 7 evolved Cfr variants, referred herein as CfrV1-V7, as representative mutational combinations for further characterization (Fig. 1C). All selected Cfr variants contain mutations in the *cfr* open reading frame while CfrV6 and CfrV7 also harbor P_{tet} alterations (Fig. 1D). Compared to CfrWT, these variants confer ~2 to ~16-fold enhanced resistance to $PhLOPS_A$ antibiotics, yet with no changes in susceptibility to trimethoprim, an antibiotic that does not inhibit the ribosome (Fig. 1E, table S4). Interestingly, the promoter alterations enable CfrV7 to be expressed and confer resistance to tiamulin in the absence of inducer (fig. S1). The robustness of resistance, and the absence of active-site mutations, suggests Cfr variants do not act as dominant-negative enzymes that inhibit C-2 methylation of A2503, as observed in a previous directed evolution experiment (*36*). Furthermore, the specificity of resistance to $PhLOPS_A$ antibiotics suggests that these Cfr variants elicit their effects through PTC modification rather than triggering a stress response that confers global resistance.

Variants exhibit increased rRNA methylation and Cfr protein production

To test the hypothesis that Cfr variants mediate higher resistance by increasing the fraction of ribosomes with m^8A2503, we evaluated the methylation status of A2503 by mass spectrometry. Specifically, we expressed Cfr in *E. coli* and used oligonucleotide protection to isolate a 40-nt fragment of 23S rRNA containing A2503. The isolated fragment was then enzymatically digested and analyzed by MALDI-TOF mass spectrometry (Fig. 2A, fig. S2-S3). As expected, an empty vector produces a 1013 m/z fragment corresponding to the mono-methylated m^2A2503,

modification installed by the endogenous enzyme RlmN. Upon expression of Cfr, we observe a reduction in the 1013 m/z peak and the emergence of a new peak at 1027 m/z, corresponding to m^2A2503 conversion into hypermethylated m^2m^8A2503. CfrWT is able to convert less than ~40% of m^2A2503 into the hypermethylated m^2m^8A2503 product. In contrast, the evolved variants achieve ~50-90% methylation of A2503, indicating that variants are more active than CfrWT *in vivo.*

The ability of evolved Cfr variants to achieve enhanced ribosome methylation *in vivo* could be attributed to enhanced enzymatic activity and/or higher levels of functional enzyme. To test the hypothesis that Cfr variants achieve higher turnover number, we anaerobically purified and reconstituted CfrWT and a representative evolved variant, CfrV4. We then evaluated the ability of CfrWT and CfrV4 to methylate a 23S rRNA fragment (2447-2625) *in vitro* by monitoring the incorporation of radioactivity from [^{3}H-methyl] *S*-adenosylmethionine (SAM) into RNA substrate under saturating conditions (*37*). However, no significant difference in k_{cat} between CfrWT ($3.45 \times 10^{-2} \pm 3.2 \times 10^{-3}$ min^{-1}) and CfrV4 ($2.25 \times 10^{-2} \pm 1.3 \times 10^{-3}$ min^{-1}) was observed (fig. S4).

Given the above, we hypothesized that the variants might alter protein levels. To monitor Cfr protein levels, we inserted a flexible linker followed by a C-terminal FLAG tag, which we confirmed does not alter resistance (table S5). Interestingly, immunoblotting against FLAG revealed that in addition to full-length Cfr, N-terminally truncated Cfr proteins are also produced (Fig. 2B). The truncations result from translation initiation at internal methionines but do not contribute to resistance (fig. S5), indicating they are likely non-functional enzymes unable to methylate A2503. Interestingly the larger molecular weight truncation is present only in CfrV1/V4/V6 and is generated by the I26M mutation introduced during directed evolution. Quantification of resistance-causative, full-length Cfr proteins alone revealed that the evolved variants achieve ~20-100-fold higher steady-state protein levels than CfrWT (Fig. 2B).

We measured transcript levels for all variants to assess contribution of altered transcription to increased protein levels. For Cfr variants with promoter alterations, enhanced production of the Cfr transcript is a large contributor to Cfr protein expression, as CfrV6 and CfrV7 exhibit ~6 and ~10-fold enhancement in Cfr mRNA levels compared to CfrWT, respectively (Fig. 2C). However, the ~2 to 3-fold increase in mRNA levels for CfrV1-5 cannot explain the multi-fold improvement in protein expression and indicates that these variants also boost protein production through a post-transcriptional process. This is further supported by the expression profiles for CfrV1-5, which are dominated by the full-length protein (fig. S6). Interestingly, enhanced production of Cfr protein correlates with larger fitness defects in *E. coli*, with an increase in doubling time of ~4 min for CfrV7 compared to empty vector in the absence of antibiotics (Fig. 2D).

Mutations in the promoter and second amino acid residue of Cfr drive resistance and expression

Given that the evolved variants achieve robust enhancement in Cfr expression we sought to elucidate the mechanism(s) by which this occurs. To evaluate the importance of promoter alterations, we generated a construct where the P_{tet}* promoter sequence from CfrV6 was inserted upstream of CfrWT open reading frame, herein referred to as P_{tet}*V6-CfrWT. The insertion of P_{tet}* alone was sufficient to elicit improvement in Cfr expression (Fig. 3A). Furthermore, *E. coli*

expressing P_{tet}*V6-CfrWT resembled CfrV6 in its ability to survive in the presence of chloramphenicol (Fig. 3B). Together, these results suggest the altered promoter drives expression and resistance for CfrV6.

To investigate the contributions of mutations within the Cfr protein, we generated constructs containing Cfr mutations N2K/I, I26M, and S39G in isolation. Interestingly, we observe that mutations at the second position, N2K and N2I, display the largest enhancements in expression, ~27-fold and ~12-fold respectively (Fig. 3A). The dominance of the second position mutants is further manifested in *E. coli* expressing CfrN2K, but not I26M or S39G, exhibiting similar survival in the presence of chloramphenicol to that of the triple mutant, CfrV3 (Fig. 3C). Similarly, *E. coli* expressing CfrN2I also exhibits increased resistance to chloramphenicol when compared to the corresponding directed evolution variant, CfrV5, albeit weaker than CfrN2K (fig. S7). Together, these results suggest that the second position mutations drive the robust expression and resistance observed for CfrV1-5. Of note, ribosome methylation by the produced Cfr does not impact the translation of CfrN2K, as this mutant and it's corresponding catalytically inactive double mutant protein CfrN2K_C338A are similarly highly expressed (fig. S8).

Mutations impact Cfr translation and degradation

The Cfr coding mutations drive enhanced steady-state protein levels of Cfr protein through a post-transcriptional process. However, because levels at steady-state reflect the net effect of protein synthesis and degradation, we sought to evaluate how Cfr mutations impact both processes, especially since the nature of N-terminal amino acids and codons can greatly influence both translation and degradation in bacteria (*38–49*).

To test the hypothesis that second position mutations enhance translation of mutants, we used polysome profiling to evaluate the relative abundance of Cfr mRNA in polysome fractions. Polysome profiles derived from 10-55% sucrose gradients appear similar across biological conditions, suggesting expression of CfrWT and its evolved mutants do not affect global translation (Fig. 4, A and B). CfrWT transcripts migrate with low polysomes (fractions 10, 11) (Fig. 4C). In contrast, CfrV4 transcripts are strongly shifted toward high polysomes (fractions 16, 17), which indicate that CfrV4 mRNA is associated with a large quantity of ribosomes and is better translated than CfrWT (Fig. 4D). Further support that CfrV4 is well-translated is the observation that CfrV4 mRNA co-migrates with mRNA of the well-translated housekeeping gene, *recA (50)* (fig. S9). At least in part, this is due to the N2K mutation which shifts transcripts to higher polysomes fractions (fractions 12, 13) (Fig. 4C). The *recA* control mRNA shows excellent reproducibility across biological samples, indicating that the observed shift of mutant Cfr transcripts towards higher polysomes is due to introduced mutations (Fig. 4B). Taken together, these results suggest that enhanced translation is a cumulative effect of N2K and other ORF mutations obtained by directed evolution.

To further interrogate the role of second position mutations in Cfr translation, we determined the second codon identity for all sequenced variants from the final rounds of evolution (table S2). Interestingly, all N2K mutations were encoded by an AAA codon, while AUU encoded all N2I mutations. In *E. coli,* the tRNA molecules that decode K(AAA) and I(AUU) are slightly more abundant than the *wild-type* N(AAU), accounting for 3.0% and 5.4% of the tRNA pool compared to 1.9%, respectively (*51*). To test if tRNA abundance and codon sequence contribute to enhanced translation, we evaluated the impact of synonymous codons on protein expression.

Lysine codons AAA and AAG are decoded by the same $tRNA^{Lys}$ in *E. coli.* Interestingly, mutating CfrN2K from AAA to AAG, which increases G/C content, did not significantly impact expression (fig. S10). The isoleucine AUA codon is decoded by the low-abundant $tRNA^{Ile2}$ (*52*, *53*). Mutation of N2I from AUU to the AUA rare codon resulted in a ~2-fold decrease in Cfr expression, supporting tRNA abundance as a contributing factor (fig. S10).

To evaluate impact of mutations introduced during directed evolution on protein half-life, we monitored changes in protein abundance over time after halting expression with rifampicin (Fig. 4E, fig. S11). While CfrWT is rapidly degraded with a half-life of ~20 min, CfrN2K/I exhibit increased half-lives of ~60 min. These results suggest that mutation of the second amino acid to lysine or isoleucine contribute to improved steady-state expression both by enhancing translation and stability of Cfr in the cell. CfrS39G also exhibits an increased half-life of ~60 min. The half-life increase is the most pronounced for the I26M single point mutant and similar to that of the triple-mutant, CfrV3 (>100 min for both proteins). Together, these results suggest that evolved variants achieve higher expression through mutations that both enhance translation and decrease degradation of mutant Cfr proteins.

Evolved Cfr variant enables understanding of the structural basis of Cfr resistance

Molecular understanding of Cfr-mediated resistance to antibiotics necessitates structural insights into methylated ribosomes. However, obtaining the structure of Cfr-modified ribosome has been so far hampered by moderate methylation efficiency of *S. aureus* Cfr, a challenge that can be addressed by the improved methylation ability of directed evolution variants. Of all characterized evolved variants, CfrV7 achieves highest levels of antibiotic resistance and methylation of rRNA, providing a unique tool for structural determination. Relative peak quantification of the MALDI spectra revealed that CfrV7 achieved near-stoichiometric (~90%) m^8A2503 methylation (fig. S3).

Ribosomes were purified from *E. coli* expressing CfrV7 to obtain a 2.2Å cryo-EM structure of the Cfr-modified 50S ribosomal subunit (Fig. 5A, fig. S12, table S6). The high resolution cryo-EM density map enabled modeling all known modified nucleotides including the novel C8 methylation of A2503 (Fig. 5B). Furthermore, comparison of the Cfr-modified ribosome with the high resolution cryo-EM structure of unmodified, *wild-type* ribosome we published previously (*33*) allowed us to identify with high confidence any structural changes due to the presence of m^8A2503. Importantly, modification of A2503 by Cfr does not affect the conformation or position of the A2503 nucleotide. The adenine ring remains in the *syn*-conformation and places the newly installed C8-methyl group directly into the PTC to sterically obstruct antibiotic binding (Fig. 5, C and D).

Strikingly, beyond the addition of a single methyl group to the substrate nucleotide, presence of m^8A2503 does not result in any additional structural changes to the PTC region of the ribosome (Fig. 5C). Furthermore, the increased resistance provided by CfrV7 appears to be mediated specifically by improved methylation of A2503. No off-target activity of the evolved variant was observed as manual inspection did not reveal density that could correspond to additional C8-methyl adenosines within the high-resolution regions of the 50S ribosomal subunit. This result was cross-validated using our qPTxM tool (*33*), which identified only A2503 and A556 as possible C8-methyl adenosines. Closer examination of A556 reveals it registered as a false positive (fig. S13).

Contrary to previous reports, we do not observe changes to methylation of C2498, a distal PTC nucleotide whose endogenous 2'-O-ribose modification has previously been reported to be suppressed by Cfr methylation of A2503 and hypothesized to alter the PTC through long-range effects (*7*, *8*, *54*). Although it is unclear what percentage of C2498 retains the native modification in our structure, we observe clear density for the methyl group and the nucleotide conformation is unaltered. The density for the methyl group is slightly off of the rotameric position, but the dropoff in density along the methyl bond matches the expected shape (fig. S13). Together, the results do not indicate that conformational changes to C2498 are involved in Cfr-mediated resistance.

Structural overlay of the Cfr-modified ribosome with existing structures of ribosomes-antibiotic complexes enables direct identification of chemical moieties responsible for steric collision with m^8A2503 (fig. S14). For example, the pleuromutilin class of PTC-targeting antibiotics have recently regained interest for their applications as antimicrobial agents in humans (*55*). Overlay of bacterial ribosomes in complex with the pleuromutilin derivative tiamulin, the selection antibiotic used during directed evolution, reveals steric clash between C10 alkyl substituent and the C11 hydroxyl group of the antibiotic with the Cfr-introduced methyl group (Fig. 5D). Given recent synthetic advances that enable more extensive modification of the pleuromutilin scaffold (*56*, *57*), these results will inform design of next-generation antibiotics that can overcome Cfr-mediated resistance.

Discussion

By relying on directed evolution under antibiotic selection, we identified strategies that increase the ability of a multi-antibiotic resistance determinant Cfr to cause resistance. Enhanced resistance is associated with improved *in vivo* methylation of rRNA at m^8A2503. The positive correlation between extent of rRNA modification and resistance aligns with previous studies that investigated linezolid resistance caused by mutation of rRNA, where the severity of linezolid resistance was proportional to the number of 23S rRNA alleles harboring the resistance mutation (*58–60*). While alteration of the antibiotic binding site through mutations and enzymatic modification of 23S rRNA are functionally distinct, dependence on the extent of rRNA modification provides parallels between the two mechanisms. Although Cfr-mediated methylation is an enzymatic process, the ability of Cfr to confer resistance is restricted by ribosome assembly. Since the A2503 is only accessible to Cfr prior to incorporation of 23S rRNA into the large ribosomal subunit (*10*), the extent of resistance correlates with the ability of the enzyme to methylate 23S rRNA prior to its incorporation into the 50S subunit. The results of our evolution experiment indicate that increasing the intracellular concentrations of Cfr, rather than improving catalysis of an enzyme with a complex radical mechanism (*11*, *37*, *61*, *62*) is the preferred strategy to increase the proportion of ribosomes with the protective m^8A2503 modification.

The evolved Cfr variants improve expression using two mechanisms. Improved Cfr expression for CfrV6/7 is driven by increased transcription due to alterations to the P_{tet} promoter likely introduced by primer slippage during the error-prone PCR step of directed evolution. CfrV6 contains a full duplication of P_{tet}, providing two sites for transcription initiation, likely responsible for enhanced *cfr* transcript levels. Interestingly, this result parallels a clinical instance of high Cfr resistance discovered in a *S. epidermidis* isolate where transcription of *cfr* was driven

by two promoters (*63*) and highlights transcriptional regulation as an important mechanism for modulating the *in vivo* activity of Cfr.

Improved expression for evolved variants CfrV1-5 is mediated by mutations that improve both translational efficiency and protein stability *in vivo*. Of the tested mutations, I26M provides the largest improvement in stability. Of note, the N-terminally truncated Cfr derived from translation initiation at I26M is rapidly degraded, as no detectable protein is observed after 60 min (Fig. 4E). However, these results indicate that the costly production and clearance of this nonfunctional protein is offset by the improved cellular stability of the full-length Cfr provided by the I26M mutation. Of the mutations investigated, N2K is the largest contributor to enhanced Cfr expression and resistance. Although N2K contributes to cellular stability, our results suggest that improved Cfr translation is the dominant role of this mutation. The influence of N-terminal residues on early stages of translation has been well documented, with several proposed models to explain how tRNA abundance, local mRNA sequence and structure, amino acid composition of the nascent chain, and interaction between the mRNA or the nascent chain and the ribosome itself influence translation initiation and elongation (*39–44*, *64–68*). Although the mechanism is poorly understood, the presence of an AAA codon after the start codon is associated with improved translation efficiency (*45–49*, *69*, *70*). Interestingly, the observed internal translation start sites (I26M, M95) that are responsible for producing Cfr truncations (Fig. 2B, fig. S5) contain a lysine immediately after methionine, further highlighting the putative role for lysine codons in early steps of translation.

To date, only a few *S. aureus* Cfr variants have been reported and no mutations matching those obtained from directed evolution have been found in clinical isolates. However, enhanced expression through positioning of Lys as the second amino acid of Cfr can be recapitulated by accessing an upstream translational start site found in a native sequence context of *cfr* (fig. S15). In the specific case of the pSCFS1 resistance plasmid from a natural isolate, the sequence upstream of the annotated start codon, which we validated as the site of initiation under the experimental conditions tested (fig. S16), contains regulatory elements that have been proposed to modulate Cfr expression (*6*, *71*). It is plausible that in response to antibiotics, translation initiation at the upstream start codon would result in the addition of three amino acids (MKE) to the N-terminus of Cfr and thus placement of a lysine (K) at position two, analogous to the N2K mutation. Although experimental evidence for start codon selection as a Cfr inducibility mechanism requires further investigation, N-terminal addition of MKE to Cfr expressed under non-native promoter in pZA phenocopies the N2K directed evolution mutation, resulting in improved Cfr expression (~20-fold) and higher resistance to chloramphenicol compared to CfrWT (fig. S15). We speculate that bacteria may ramp expression of Cfr by using the upstream start codon in response to antibiotic pressure. Since our assessment of the evolved variants indicates that an increase in Cfr expression is accompanied by a decrease in fitness (Fig. 2D), start site selection in response to antibiotic pressure would mitigate detrimental impact on fitness while enabling higher resistance when acutely needed.

In addition to identifying mechanisms that increase Cfr-mediated resistance, directed evolution of Cfr also provided an indispensable reagent that enabled structural determination of the Cfr-modified ribosome. The high-resolution cryo-EM structure revealed that broad resistance is due to steric effects of the judiciously positioned methyl group within the shared binding site of PTC-targeting antibiotics. Lack of notable changes in position or orientation of A2503 or surrounding PTC nucleotides upon Cfr methylation suggests that the resulting modification does

not obstruct the translation capabilities of the ribosome. This absence of PTC disruption is consistent with the observation that the fitness cost of Cfr acquisition is not due to ribosome modification, but rather results from expression of the exogenous protein (*28*). Importantly, overlay with existing structures containing PTC-targeting antibiotics provides direct visualization of chemical moieties that are sterically impacted by m^8A2503 and will inform design of antibiotic derivatives that can overcome resistance mediated by Cfr.

References

1. T. Tenson, A. Mankin, Antibiotics and the ribosome. *Mol. Microbiol.* **59**, 1664–1677 (2006).

2. D. N. Wilson, The A–Z of bacterial translation inhibitors. *Critical Reviews in Biochemistry and Molecular Biology*. **44** (2009), pp. 393–433.

3. S. Arenz, D. N. Wilson, Blast from the Past: Reassessing Forgotten Translation Inhibitors, Antibiotic Selectivity, and Resistance Mechanisms to Aid Drug Development. *Mol. Cell*. **61**, 3–14 (2016).

4. B. Vester, K. S. Long, *Antibiotic Resistance in Bacteria Caused by Modified Nucleosides in 23S Ribosomal RNA* (Landes Bioscience, 2013).

5. D. N. Wilson, Ribosome-targeting antibiotics and mechanisms of bacterial resistance. *Nat. Rev. Microbiol.* **12**, 35–48 (2014).

6. S. Schwarz, C. Werckenthin, C. Kehrenberg, Identification of a Plasmid-Borne Chloramphenicol-Florfenicol Resistance Gene inStaphylococcus sciuri. *Antimicrob. Agents Chemother.* **44**, 2530–2533 (2000).

7. C. Kehrenberg, S. Schwarz, L. Jacobsen, L. H. Hansen, B. Vester, A new mechanism for chloramphenicol, florfenicol and clindamycin resistance: methylation of 23S ribosomal RNA at A2503. *Mol. Microbiol.* **57**, 1064–1073 (2005).

8. A. M. B. Giessing, S. S. Jensen, A. Rasmussen, L. H. Hansen, A. Gondela, K. Long, B. Vester, F. Kirpekar, Identification of 8-methyladenosine as the modification catalyzed by the radical SAM methyltransferase Cfr that confers antibiotic resistance in bacteria. *RNA*. **15**, 327–336 (2009).

9. K. H. Kaminska, E. Purta, L. H. Hansen, J. M. Bujnicki, B. Vester, K. S. Long, Insights into the structure, function and evolution of the radical-SAM 23S rRNA methyltransferase Cfr that confers antibiotic resistance in bacteria. *Nucleic Acids Res.* **38**, 1652–1663 (2010).

10. F. Yan, J. M. LaMarre, R. Röhrich, J. Wiesner, H. Jomaa, A. S. Mankin, D. G. Fujimori, RlmN and Cfr are radical SAM enzymes involved in methylation of ribosomal RNA. *J. Am. Chem. Soc.* **132**, 3953–3964 (2010).

11. F. Yan, D. G. Fujimori, RNA methylation by radical SAM enzymes RlmN and Cfr proceeds via methylene transfer and hydride shift. *Proc. Natl. Acad. Sci. U. S. A.* **108**, 3930–3934 (2011).

12. T. L. Grove, J. S. Benner, M. I. Radle, J. H. Ahlum, B. J. Landgraf, C. Krebs, S. J. Booker, A Radically Different Mechanism for S-Adenosylmethionine-Dependent Methyltransferases. *Science*. **332** (2011), pp. 604–607.

13. K. S. Long, J. Poehlsgaard, C. Kehrenberg, S. Schwarz, B. Vester, The Cfr rRNA

methyltransferase confers resistance to Phenicols, Lincosamides, Oxazolidinones, Pleuromutilins, and Streptogramin A antibiotics. *Antimicrob. Agents Chemother.* **50**, 2500–2505 (2006).

14. L. K. Smith, A. S. Mankin, Transcriptional and translational control of the mlr operon, which confers resistance to seven classes of protein synthesis inhibitors. *Antimicrob. Agents Chemother.* **52**, 1703–1712 (2008).

15. Y. S. Polikanov, A. L. Starosta, M. F. Juette, R. B. Altman, D. S. Terry, W. Lu, B. J. Burnett, G. Dinos, K. A. Reynolds, S. C. Blanchard, T. A. Steitz, D. N. Wilson, Distinct tRNA Accommodation Intermediates Observed on the Ribosome with the Antibiotics Hygromycin A and A201A. *Mol. Cell*. **58**, 832–844 (2015).

16. S.-M. Toh, L. Xiong, C. A. Arias, M. V. Villegas, K. Lolans, J. Quinn, A. S. Mankin, Acquisition of a natural resistance gene renders a clinical strain of methicillin-resistant Staphylococcus aureus resistant to the synthetic antibiotic linezolid. *Mol. Microbiol.* **64**, 1506–1514 (2007).

17. C. A. Arias, M. Vallejo, J. Reyes, D. Panesso, J. Moreno, E. Castañeda, M. V. Villegas, B. E. Murray, J. P. Quinn, Clinical and microbiological aspects of linezolid resistance mediated by the cfr gene encoding a 23S rRNA methyltransferase. *J. Clin. Microbiol.* **46**, 892–896 (2008).

18. J. Shen, Y. Wang, S. Schwarz, Presence and dissemination of the multiresistance gene cfr in Gram-positive and Gram-negative bacteria. *J. Antimicrob. Chemother.* **68**, 1697–1706 (2013).

19. B. Vester, The cfr and cfr-like multiple resistance genes. *Res. Microbiol.* **169**, 61–66 (2018).

20. G. Morales, J. J. Picazo, E. Baos, F. J. Candel, A. Arribi, B. Peláez, R. Andrade, M.-A. de la Torre, J. Fereres, M. Sánchez-García, Resistance to linezolid is mediated by the cfr gene in the first report of an outbreak of linezolid-resistant Staphylococcus aureus. *Clin. Infect. Dis.* **50**, 821–825 (2010).

21. J. B. Locke, G. Morales, M. Hilgers, K. G C, S. Rahawi, J. José Picazo, K. J. Shaw, J. L. Stein, Elevated linezolid resistance in clinical cfr-positive Staphylococcus aureus isolates is associated with co-occurring mutations in ribosomal protein L3. *Antimicrob. Agents Chemother.* **54**, 5352–5355 (2010).

22. H. Bonilla, M. D. Huband, J. Seidel, H. Schmidt, M. Lescoe, S. P. McCurdy, M. M. Lemmon, L. A. Brennan, A. Tait-Kamradt, L. Puzniak, J. P. Quinn, Multicity outbreak of linezolid-resistant Staphylococcus epidermidis associated with clonal spread of a cfr-containing strain. *Clin. Infect. Dis.* **51**, 796–800 (2010).

23. J. C. Cai, Y. Y. Hu, H. W. Zhou, G.-X. Chen, R. Zhang, Dissemination of the same cfr-carrying plasmid among methicillin-resistant Staphylococcus aureus and coagulase-negative staphylococcal isolates in China. *Antimicrob. Agents Chemother.* **59**, 3669–3671 (2015).

24. F. Layer, S. Vourli, V. Karavasilis, B. Strommenger, K. Dafopoulou, A. Tsakris, G. Werner, S. Pournaras, Dissemination of linezolid-dependent, linezolid-resistant Staphylococcus epidermidis clinical isolates belonging to CC5 in German hospitals. *J. Antimicrob. Chemother.* **73**, 1181–1184 (2018).

25. A. Lazaris, D. C. Coleman, A. M. Kearns, B. Pichon, P. M. Kinnevey, M. R. Earls, B. Boyle, B. O'Connell, G. I. Brennan, A. C. Shore, Novel multiresistance cfr plasmids in linezolid-resistant methicillin-resistant Staphylococcus epidermidis and vancomycin-resistant Enterococcus faecium (VRE) from a hospital outbreak: co-location of cfr and optrA in VRE. *J. Antimicrob. Chemother.* **72**, 3252–3257 (2017).

26. L. Dortet, P. Glaser, N. Kassis-Chikhani, D. Girlich, P. Ichai, M. Boudon, D. Samuel, E. Creton, D. Imanci, R. Bonnin, N. Fortineau, T. Naas, Long-lasting successful dissemination of resistance to oxazolidinones in MDR Staphylococcus epidermidis clinical isolates in a tertiary care hospital in France. *J. Antimicrob. Chemother.* **73**, 41–51 (2018).

27. C. Weßels, B. Strommenger, I. Klare, J. Bender, S. Messler, F. Mattner, M. Krakau, G. Werner, F. Layer, Emergence and control of linezolid-resistant Staphylococcus epidermidis in an ICU of a German hospital. *J. Antimicrob. Chemother.* **73**, 1185–1193 (2018).

28. J. M. LaMarre, J. B. Locke, K. J. Shaw, A. S. Mankin, Low fitness cost of the multidrug resistance gene cfr. *Antimicrob. Agents Chemother.* **55**, 3714–3719 (2011).

29. S. Schwarz, J. Shen, K. Kadlec, Y. Wang, G. Brenner Michael, A. T. Feßler, B. Vester, Lincosamides, Streptogramins, Phenicols, and Pleuromutilins: Mode of Action and Mechanisms of Resistance. *Cold Spring Harb. Perspect. Med.* **6** (2016), doi:10.1101/cshperspect.a027037.

30. S.-M. Toh, L. Xiong, T. Bae, A. S. Mankin, The methyltransferase YfgB/RlmN is responsible for modification of adenosine 2503 in 23S rRNA. *RNA*. **14**, 98–106 (2008).

31. F. Schlünzen, R. Zarivach, J. Harms, A. Bashan, A. Tocilj, R. Albrecht, A. Yonath, F. Franceschi, Structural basis for the interaction of antibiotics with the peptidyl transferase centre in eubacteria. *Nature*. **413**, 814–821 (2001).

32. D. Tu, G. Blaha, P. B. Moore, T. A. Steitz, Structures of MLSBK antibiotics bound to mutated large ribosomal subunits provide a structural explanation for resistance. *Cell*. **121**, 257–270 (2005).

33. V. Stojković, A. G. Myasnikov, I. D. Young, A. Frost, J. S. Fraser, D. G. Fujimori, Assessment of the nucleotide modifications in the high-resolution cryo-electron microscopy structure of the Escherichia coli 50S subunit. *Nucleic Acids Res.* **48**, 2723–2732 (2020).

34. M. Barlow, B. G. Hall, Experimental prediction of the natural evolution of antibiotic resistance. *Genetics*. **163**, 1237–1241 (2003).

35. A. Wellner, M. Raitses Gurevich, D. S. Tawfik, Mechanisms of protein sequence divergence and incompatibility. *PLoS Genet.* **9**, e1003665 (2013).

36. V. Stojković, L. Noda-Garcia, D. S. Tawfik, D. G. Fujimori, Antibiotic resistance evolved via inactivation of a ribosomal RNA methylating enzyme. *Nucleic Acids Res.* **44**, 8897–8907 (2016).

37. M. R. Bauerle, T. L. Grove, S. J. Booker, Investigation of Solvent Hydron Exchange in the Reaction Catalyzed by the Antibiotic Resistance Protein Cfr. *Biochemistry*. **57**, 4431–4439 (2018).

38. S. Gottesman, Proteolysis in bacterial regulatory circuits. *Annu. Rev. Cell Dev. Biol.* **19**, 565–587 (2003).

39. S. Bhattacharyya, W. M. Jacobs, B. V. Adkar, J. Yan, W. Zhang, E. I. Shakhnovich, Accessibility of the Shine-Dalgarno Sequence Dictates N-Terminal Codon Bias in E. coli. *Mol. Cell*. **70**, 894–905.e5 (2018).

40. K. Bentele, P. Saffert, R. Rauscher, Z. Ignatova, N. Blüthgen, Efficient translation initiation dictates codon usage at gene start. *Mol. Syst. Biol.* **9**, 675 (2013).

41. T. Tuller, A. Carmi, K. Vestsigian, S. Navon, Y. Dorfan, J. Zaborske, T. Pan, O. Dahan, I. Furman, Y. Pilpel, An evolutionarily conserved mechanism for controlling the efficiency of protein translation. *Cell*. **141**, 344–354 (2010).

42. M. Verma, J. Choi, K. A. Cottrell, Z. Lavagnino, E. N. Thomas, S. Pavlovic-Djuranovic, P. Szczesny, D. W. Piston, H. S. Zaher, J. D. Puglisi, S. Djuranovic, A short translational ramp determines the efficiency of protein synthesis. *Nat. Commun.* **10**, 5774 (2019).

43. D. B. Goodman, G. M. Church, S. Kosuri, Causes and Effects of N-Terminal Codon Bias in Bacterial Genes. *Science*. **342** (2013), pp. 475–479.

44. G. Boël, R. Letso, H. Neely, W. N. Price, K.-H. Wong, M. Su, J. Luff, M. Valecha, J. K. Everett, T. B. Acton, R. Xiao, G. T. Montelione, D. P. Aalberts, J. F. Hunt, Codon influence on protein expression in E. coli correlates with mRNA levels. *Nature*. **529**, 358–363 (2016).

45. A. C. Looman, J. Bodlaender, L. J. Comstock, D. Eaton, P. Jhurani, H. A. de Boer, P. H. van Knippenberg, Influence of the codon following the AUG initiation codon on the expression of a modified lacZ gene in Escherichia coli. *EMBO J.* **6**, 2489–2492 (1987).

46. C. M. Stenström, H. Jin, L. L. Major, W. P. Tate, L. A. Isaksson, Codon bias at the 3'-side of the initiation codon is correlated with translation initiation efficiency in Escherichia coli. *Gene*. **263**, 273–284 (2001).

47. C. M. Stenström, E. Holmgren, L. A. Isaksson, Cooperative effects by the initiation codon and its flanking regions on translation initiation. *Gene*. **273**, 259–265 (2001).

48. C. M. Stenström, L. A. Isaksson, Influences on translation initiation and early elongation by the messenger RNA region flanking the initiation codon at the 3' side. *Gene*. **288**, 1–8 (2002).

49. T. Sato, M. Terabe, H. Watanabe, T. Gojobori, C. Hori-Takemoto, Miura Ki, Codon and base biases after the initiation codon of the open reading frames in the Escherichia coli genome and their influence on the translation efficiency. *J. Biochem.* **129**, 851–860 (2001).

50. G.-W. Li, D. Burkhardt, C. Gross, J. S. Weissman, Quantifying Absolute Protein Synthesis Rates Reveals Principles Underlying Allocation of Cellular Resources. *Cell*. **157** (2014), pp. 624–635.

51. H. Dong, L. Nilsson, C. G. Kurland, Co-variation of tRNA Abundance and Codon Usage in Escherichia coli at Different Growth Rates. *Journal of Molecular Biology*. **260** (1996), pp. 649–663.

52. B. J. Del Tito Jr, J. M. Ward, J. Hodgson, C. J. Gershater, H. Edwards, L. A. Wysocki, F. A. Watson, G. Sathe, J. F. Kane, Effects of a minor isoleucyl tRNA on heterologous protein translation in Escherichia coli. *J. Bacteriol.* **177**, 7086–7091 (1995).

53. Y. Nakamura, T. Gojobori, T. Ikemura, Codon usage tabulated from international DNA sequence databases: status for the year 2000. *Nucleic Acids Res.* **28**, 292 (2000).

54. E. Purta, M. O'Connor, J. M. Bujnicki, S. Douthwaite, YgdE is the 2′-O-ribose methyltransferase RlmM specific for nucleotide C2498 in bacterial 23S rRNA. *Mol. Microbiol.* **72**, 1147–1158 (2009).

55. O. Goethe, A. Heuer, X. Ma, Z. Wang, S. B. Herzon, Antibacterial properties and clinical potential of pleuromutilins. *Nat. Prod. Rep.* **36**, 220–247 (2019).

56. S. K. Murphy, M. Zeng, S. B. Herzon, A modular and enantioselective synthesis of the pleuromutilin antibiotics. *Science*. **356**, 956–959 (2017).

57. E. P. Farney, S. S. Feng, F. Schäfers, S. E. Reisman, Total Synthesis of (+)-Pleuromutilin. *J. Am. Chem. Soc.* **140**, 1267–1270 (2018).

58. S. Besier, A. Ludwig, J. Zander, V. Brade, T. A. Wichelhaus, Linezolid resistance in Staphylococcus aureus: gene dosage effect, stability, fitness costs, and cross-resistances. *Antimicrob. Agents Chemother.* **52**, 1570–1572 (2008).

59. N. Ebihara, S. Hitomi, M. Goto, H. Koganemaru, Y. Sekiguchi, Recovery of linezolid-resistant, methicillin-susceptible Staphylococcus aureus in a case of implanted pacemaker-associated infection. *JMM Case Reports*. **1**, e001297 (2014).

60. M. Lobritz, R. Hutton-Thomas, S. Marshall, L. B. Rice, Recombination proficiency influences frequency and locus of mutational resistance to linezolid in Enterococcus faecalis. *Antimicrob. Agents Chemother.* **47**, 3318–3320 (2003).

61. K. P. McCusker, K. F. Medzihradszky, A. L. Shiver, R. J. Nichols, F. Yan, D. A. Maltby, C. A. Gross, D. G. Fujimori, Covalent intermediate in the catalytic mechanism of the radical S-adenosyl-L-methionine methyl synthase RlmN trapped by mutagenesis. *J. Am. Chem. Soc.* **134**, 18074–18081 (2012).

62. T. L. Grove, J. S. Benner, M. I. Radle, J. H. Ahlum, A radically different mechanism for S-adenosylmethionine–dependent methyltransferases (2011) (available at https://science.sciencemag.org/content/332/6029/604.abstract?casa_token=1IcWmuxVodkAAAAA:CG469QkMHSN05fK4KrgdCDqehQSXHma2fQec-NfQlVCQtBTy9Y6_sbZFLWLhOn6f-8eBefC-SCTep4A).

63. J. LaMarre, R. E. Mendes, T. Szal, S. Schwarz, R. N. Jones, A. S. Mankin, The genetic environment of the cfr gene and the presence of other mechanisms account for the very high linezolid resistance of Staphylococcus epidermidis isolate 426-3147L. *Antimicrob. Agents Chemother.* **57**, 1173–1179 (2013).

64. T. E. Gorochowski, Z. Ignatova, R. A. L. Bovenberg, J. A. Roubos, Trade-offs between tRNA abundance and mRNA secondary structure support smoothing of translation elongation rate. *Nucleic Acids Res.* **43**, 3022–3032 (2015).

65. G. Kudla, A. W. Murray, D. Tollervey, J. B. Plotkin, Coding-sequence determinants of gene expression in Escherichia coli. *Science*. **324**, 255–258 (2009).

66. T. Tuller, Y. Y. Waldman, M. Kupiec, E. Ruppin, Translation efficiency is determined by both codon bias and folding energy. *Proc. Natl. Acad. Sci. U. S. A.* **107**, 3645–3650 (2010).

67. G. Cambray, J. C. Guimaraes, A. P. Arkin, Evaluation of 244,000 synthetic sequences reveals design principles to optimize translation in Escherichia coli. *Nat. Biotechnol.* **36**, 1005–1015 (2018).

68. A. Riba, N. Di Nanni, N. Mittal, E. Arhné, A. Schmidt, M. Zavolan, Protein synthesis rates and ribosome occupancies reveal determinants of translation elongation rates. *Proc. Natl. Acad. Sci. U. S. A.* **116**, 15023–15032 (2019).

69. Y. M. Zalucki, P. M. Power, M. P. Jennings, Selection for efficient translation initiation biases codon usage at second amino acid position in secretory proteins. *Nucleic Acids Res.* **35**, 5748–5754 (2007).

70. J. E. Brock, R. L. Paz, P. Cottle, G. R. Janssen, Naturally occurring adenines within mRNA coding sequences affect ribosome binding and expression in Escherichia coli. *J. Bacteriol.* **189**, 501–510 (2007).

71. C. Kehrenberg, F. M. Aarestrup, S. Schwarz, IS21-558 insertion sequences are involved in the mobility of the multiresistance gene cfr. *Antimicrob. Agents Chemother.* **51**, 483–487 (2007).

72. J. Yang, Y. Zhang, I-TASSER server: new development for protein structure and function predictions. *Nucleic Acids Res.* **43**, W174–81 (2015).

73. I. Wiegand, K. Hilpert, R. E. W. Hancock, Agar and broth dilution methods to determine the minimal inhibitory concentration (MIC) of antimicrobial substances. *Nat. Protoc.* **3**, 163–175 (2008).

74. V. Stojković, D. G. Fujimori, Radical SAM-Mediated Methylation of Ribosomal RNA. *Methods Enzymol.* **560**, 355–376 (2015).

75. T. E. Andersen, B. T. Porse, F. Kirpekar, A novel partial modification at C2501 in Escherichia coli 23S ribosomal RNA. *RNA*. **10**, 907–913 (2004).

76. K. Zhou, L. Zhou, Q. ’en Lim, R. Zou, G. Stephanopoulos, H.-P. Too, Novel reference genes for quantifying transcriptional responses of Escherichia coli to protein overexpression by quantitative PCR. *BMC Mol. Biol.* **12**, 18 (2011).

77. M. W. Pfaffl, A new mathematical model for relative quantification in real-time RT-PCR. *Nucleic Acids Res.* **29**, e45 (2001).

78. F. Mohammad, A. R. Buskirk, Protocol for Ribosome Profiling in Bacteria. *Bio Protoc*. **9** (2019), doi:10.21769/BioProtoc.3468.

79. E. S. Pringle, C. McCormick, Z. Cheng, Polysome Profiling Analysis of mRNA and Associated Proteins Engaged in Translation. *Curr. Protoc. Mol. Biol.* **125**, e79 (2019).

80. P. Mehta, P. Woo, K. Venkataraman, A. W. Karzai, in *Bacterial Regulatory RNA: Methods and Protocols*, K. C. Keiler, Ed. (Humana Press, Totowa, NJ, 2012), pp. 273–289.

81. I. Khusainov, Q. Vicens, A. Bochler, F. Grosse, A. Myasnikov, J.-F. Ménétret, J. Chicher, S. Marzi, P. Romby, G. Yusupova, M. Yusupov, Y. Hashem, Structure of the 70S ribosome from human pathogen Staphylococcus aureus. *Nucleic Acids Res.* **45**, 1026 (2017).

82. H. Khatter, A. G. Myasnikov, S. K. Natchiar, B. P. Klaholz, Structure of the human 80S ribosome. *Nature*. **520**, 640–645 (2015).

83. S. Q. Zheng, E. Palovcak, J.-P. Armache, K. A. Verba, Y. Cheng, D. A. Agard, MotionCor2: anisotropic correction of beam-induced motion for improved cryo-electron microscopy. *Nat. Methods*. **14**, 331–332 (2017).

84. K. Zhang, Gctf: Real-time CTF determination and correction. *J. Struct. Biol.* **193**, 1–12 (2016).

85. S. H. W. Scheres, RELION: implementation of a Bayesian approach to cryo-EM structure determination. *J. Struct. Biol.* **180**, 519–530 (2012).

86. A. Punjani, J. L. Rubinstein, D. J. Fleet, M. A. Brubaker, cryoSPARC: algorithms for rapid unsupervised cryo-EM structure determination. *Nat. Methods*. **14**, 290–296 (2017).

87. T. Grant, A. Rohou, N. Grigorieff, cisTEM, user-friendly software for single-particle image processing. *eLife*. **7** (2018), , doi:10.7554/elife.35383.

88. P. Emsley, B. Lohkamp, W. G. Scott, K. Cowtan, Features and development ofCoot. *Acta Crystallographica Section D Biological Crystallography*. **66** (2010), pp. 486–501.

89. P. D. Adams, P. V. Afonine, G. Bunkóczi, V. B. Chen, I. W. Davis, N. Echols, J. J. Headd, L.-W. Hung, G. J. Kapral, R. W. Grosse-Kunstleve, A. J. McCoy, N. W. Moriarty, R. Oeffner, R. J. Read, D. C. Richardson, J. S. Richardson, T. C. Terwilliger, P. H. Zwart, PHENIX: a comprehensive Python-based system for macromolecular structure solution. *Acta Crystallogr. D Biol. Crystallogr.* **66**, 213–221 (2010).

90. N. W. Moriarty, R. W. Grosse-Kunstleve, P. D. Adams, electronic Ligand Builder and Optimization Workbench (eLBOW): a tool for ligand coordinate and restraint generation. *Acta Crystallogr. D Biol. Crystallogr.* **65**, 1074–1080 (2009).

91. V. B. Chen, W. B. Arendall 3rd, J. J. Headd, D. A. Keedy, R. M. Immormino, G. J. Kapral, L. W. Murray, J. S. Richardson, D. C. Richardson, MolProbity: all-atom structure validation for macromolecular crystallography. *Acta Crystallogr. D Biol. Crystallogr.* **66**, 12–21 (2010).

92. E. F. Pettersen, T. D. Goddard, C. C. Huang, G. S. Couch, D. M. Greenblatt, E. C. Meng, T. E. Ferrin, UCSF Chimera--a visualization system for exploratory research and analysis. *J. Comput. Chem.* **25**, 1605–1612 (2004).

Acknowledgements:

We thank members of the Fujimori lab for helpful discussion and comments on the manuscript. We thank the UCSF Center for Advanced CryoEM, which is supported by the National Institutes of Health [S10OD020054 and 1S10OD021741] and the Howard Hughes Medical Institute (HHMI).

Funding:

NIAID R01 AI37270 (DGF)

NSF GRFP 1650113 (KT)

UCSF Discovery Fellows program (KT)

NIGMS F32GM133129 (IDY)

NIGMS R01GM123159 (JSF)

Sangvhi-Agarwal Innovation Award (JSF)

Author contributions:

KT conceived the research, designed and performed experiments, analyzed data, and wrote the manuscript.

VS performed directed evolution, assisted in data interpretation, model refinement, and manuscript editing.

LNG performed evolution experiments and manuscript editing.

IDY and AGM performed structural analysis.

JK and AP assisted in data acquisition and analysis.

SNF provided data interpretation of polysome analysis and manuscript editing.

AF, JSF, and DST assisted in experimental design, data interpretation, and manuscript editing.

DGF conceived and supervised the research, assisted in data interpretation, and edited the manuscript.

Competing interests: Authors declare that they have no competing interests.

Data and materials availability: Atomic coordinates have been deposited in the Protein Data Bank under accession number 7LVK, and the density map has been deposited in the EMDB under accession number 23539.

Supplementary Materials

Materials and Methods

Figs. S1 to S16

Tables S1 to S6

References (73-92)

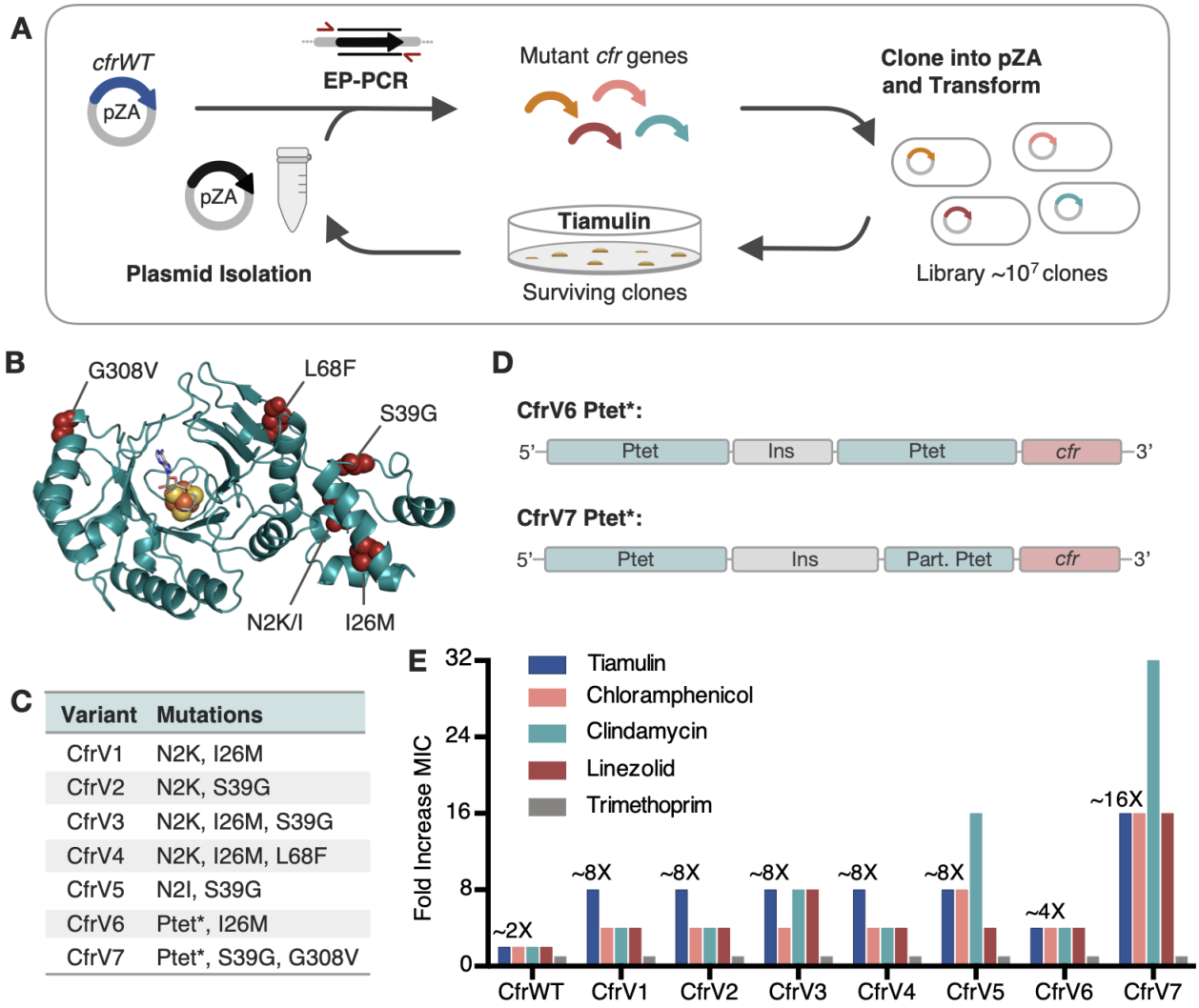

Variant	Mutations
CfrV1	N2K, I26M
CfrV2	N2K, S39G
CfrV3	N2K, I26M, S39G
CfrV4	N2K, I26M, L68F
CfrV5	N2I, S39G
CfrV6	Ptet*, I26M
CfrV7	Ptet*, S39G, G308V

Fig. 1. Evolved variants of Cfr exhibit improved resistance to PhLOPS$_A$ ribosome antibiotics. (**A**) Evolution of Cfr under selection by the PTC-targeting antibiotic tiamulin. (**B**) Cfr homology model based on RlmN generated by I-TASSER server (*72*) with mutagenic hotspots in red. Active site denoted by *S*-adenosylmethionine (grey) and [4Fe-4S] cluster (orange). (**C**) Evolved variants containing Cfr mutations selected for further study. Ptet* indicates alterations to promoter sequence. (**D**) Promoter architecture of CfrV6 and CfrV7. (**E**) Fold improvement in MIC resistance value for PhLOPS$_A$ antibiotics and trimethoprim compared to empty pZA vector control determined from three biological replicates. Trimethoprim is a negative control antibiotic that does not target the ribosome.

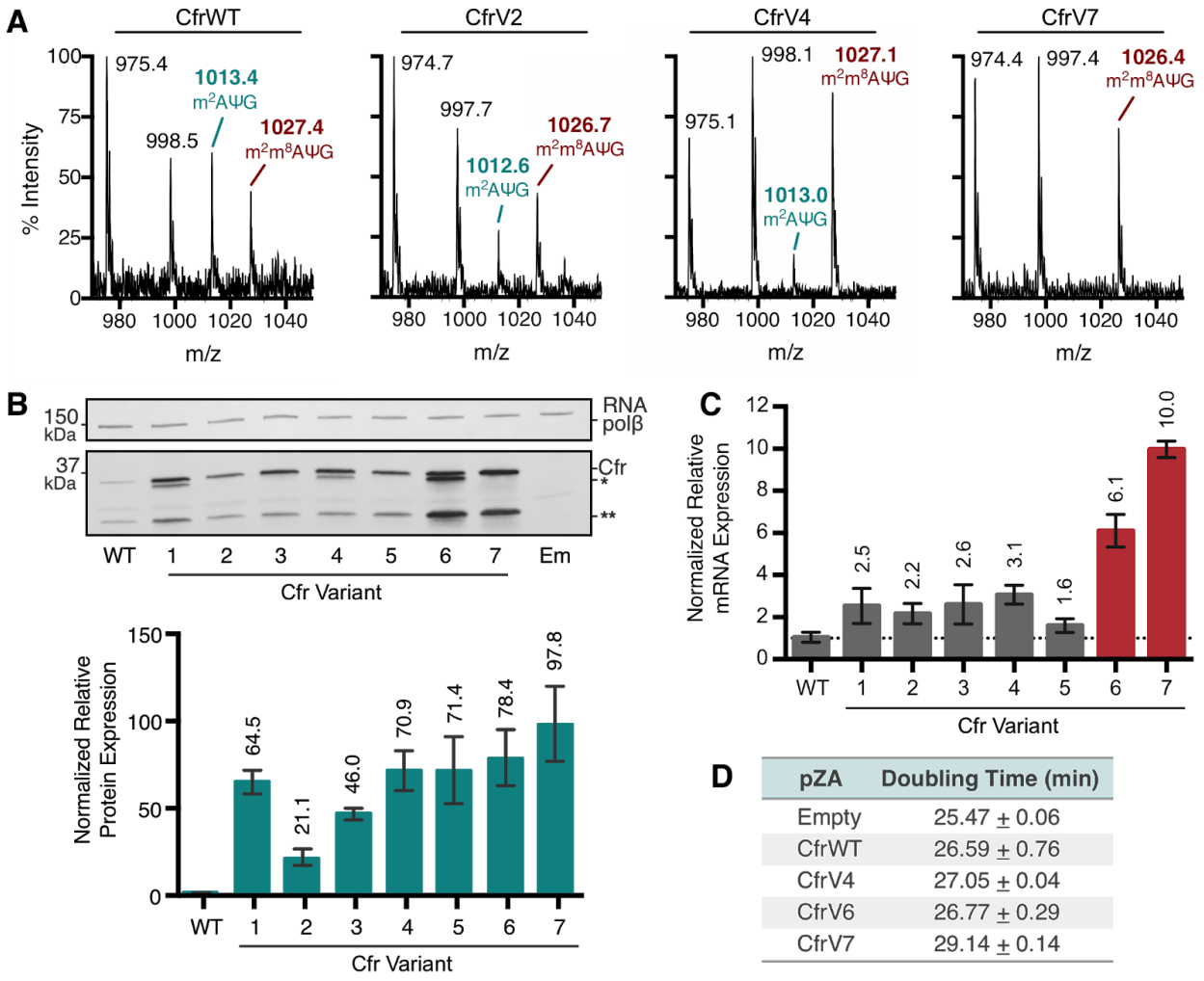

pZA	Doubling Time (min)
Empty	25.47 ± 0.06
CfrWT	26.59 ± 0.76
CfrV4	27.05 ± 0.04
CfrV6	26.77 ± 0.29
CfrV7	29.14 ± 0.14

Fig. 2. Cfr variants cause increased methylation of 23S rRNA at A2503, correlating with enhanced production of Cfr protein. (**A**) MALDI-TOF mass spectra of 23S rRNA fragments isolated from *E. coli* expressing (from left to right) CfrWT, and evolved Cfr variants V2, V4, and V7. Ψ is pseudouridine, m^2A is 2-methyladenosine, is m^2m^8A is 2,8-dimethyladenosine. Endogenously modified (m^2A2503) and Cfr-hypermodified (m^2m^8A2503) rRNA fragments correspond to m/z values of 1013 and 1027, respectively. (**B**) Relative protein expression of full-length Cfr variants compared to full-length CfrWT detected by immunoblotting against a C-terminal FLAG tag. Signal was normalized to housekeeping protein RNA polymerase β-subunit and determined from four biological replicates with standard error. Asterisks denote N-terminally truncated versions of Cfr that do not contribute to resistance. (**C**) Relative transcript levels for variants compared to CfrWT determined from three biological replicates with standard error. (**D**) Doubling times for *E. coli* expressing empty plasmid, CfrWT, or Cfr variants determined from three biological replicates with standard error.

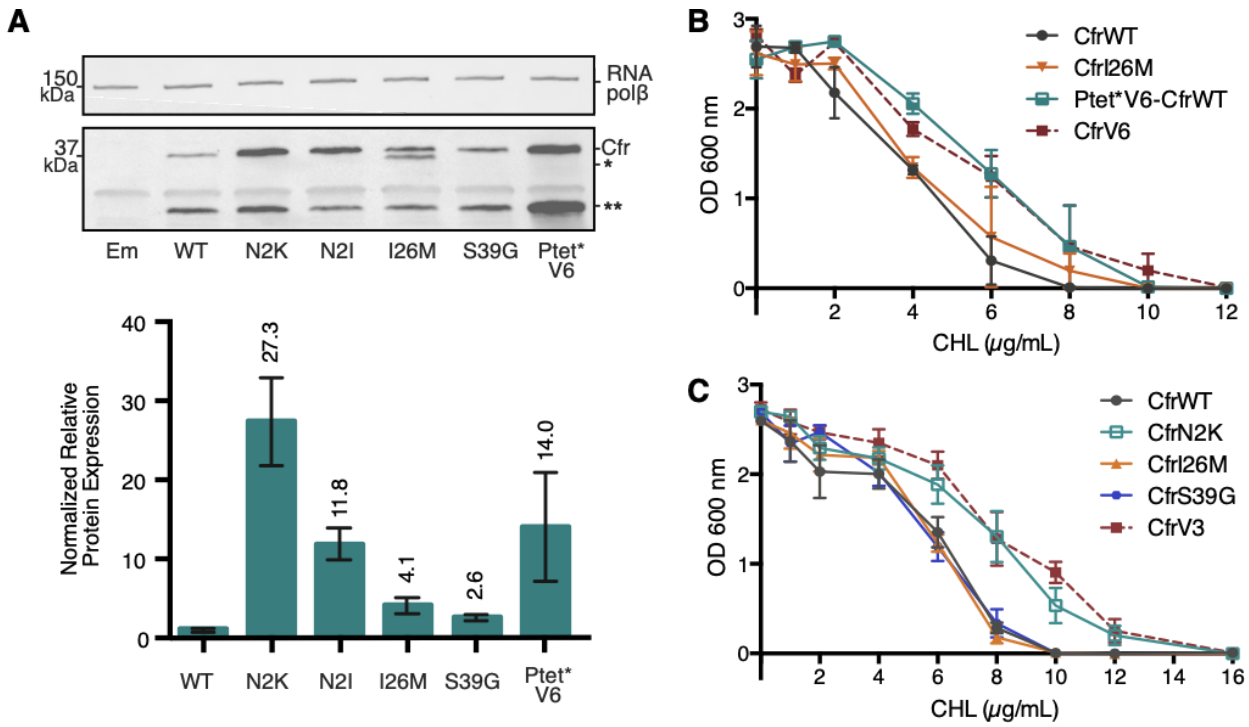

Fig. 3. Mutations to the second amino acid and promoter are the largest contributors to Cfr expression and resistance. (**A**) Effect of Cfr mutations and promoter alteration on relative Cfr protein expression was assessed by immunoblotting against a C-terminal FLAG tag. Quantification was performed for full-length Cfr protein normalized to housekeeping protein RNA polymerase β-subunit and determined from four biological replicates with standard error. Asterisks denote N-terminally truncated Cfr protein products that do not contribute to resistance and were not included in quantification. (**B**) and (**C**) Dose-dependent growth inhibition of *E. coli* expressing pZA-encoded CfrWT, CfrV6 (panel B), CfrV3 (panel C) and individual mutants that comprise these variants towards chloramphenicol (CHL) presented as an average of three biological replicates with standard error.

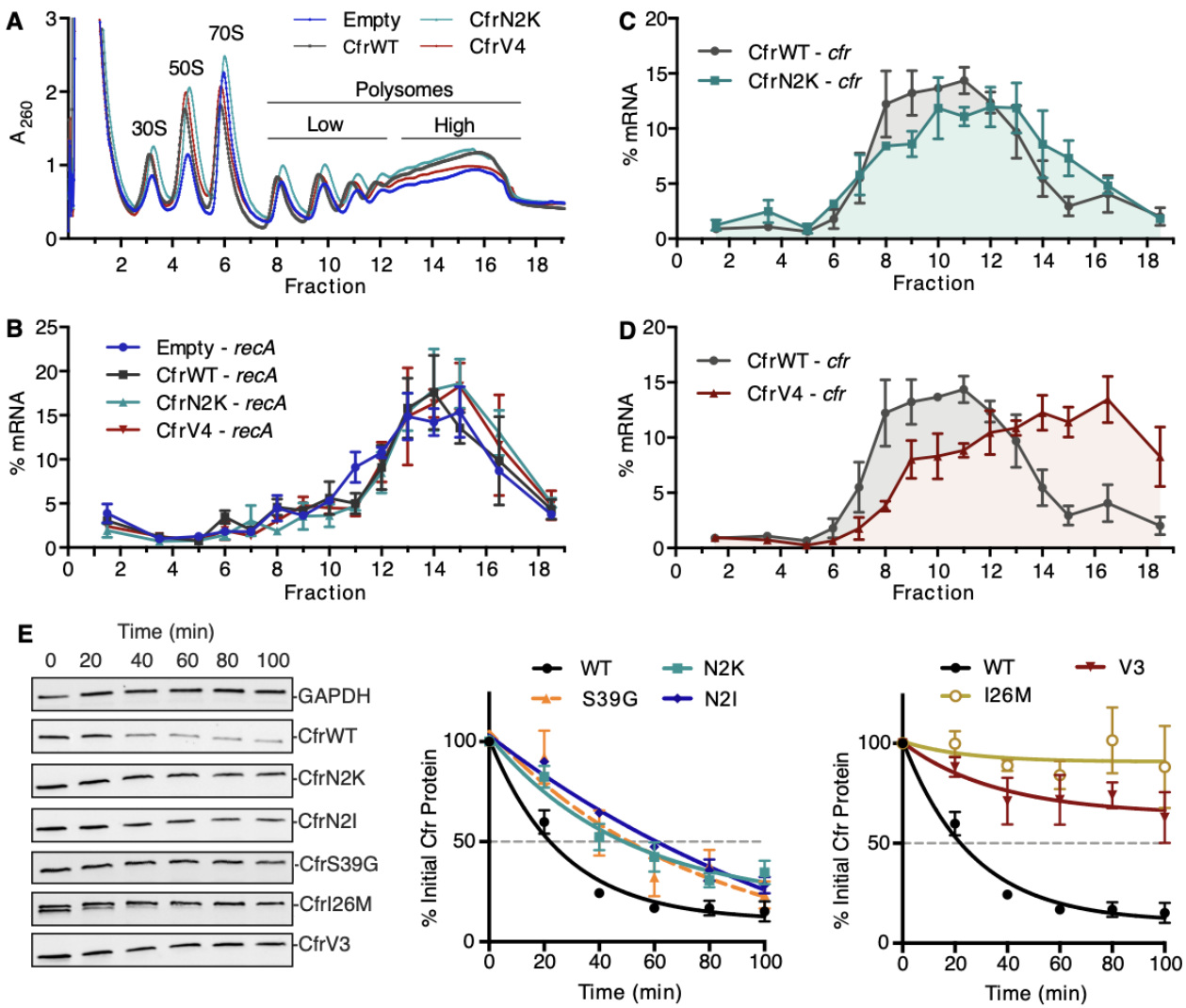

Fig. 4. Directed evolution mutations impact Cfr translation and degradation. (**A**) Sucrose gradient fractionation of polysomes from *E. coli* expressing empty vector or CfrWT/N2K/V4 denoting fractions corresponding to low- and high-density polysomes. (**B**) mRNA distribution of well-translated, housekeeping gene *recA* across polysome profiles. (**C**) mRNA distribution of Cfr transcripts expressing CfrWT or CfrN2K. (**D**) mRNA distribution of Cfr transcripts expressing CfrWT or CfrV4. For B-D, transcript levels for each fraction were determined by RT-qPCR and normalized by a luciferase mRNA control spike-in. Values presented as the average of three biological replicates with standard error. (**E**) Protein degradation kinetics of CfrWT, single mutations CfrN2K/N2I/S39G/I26M, and evolved variant CfrV3 in *E. coli* after halting expression by rifampicin treatment. Percentage of Cfr protein remaining over time was determined by immunoblotting against C-terminal FLAG tag and presented as the average of three biological replicates with standard error.

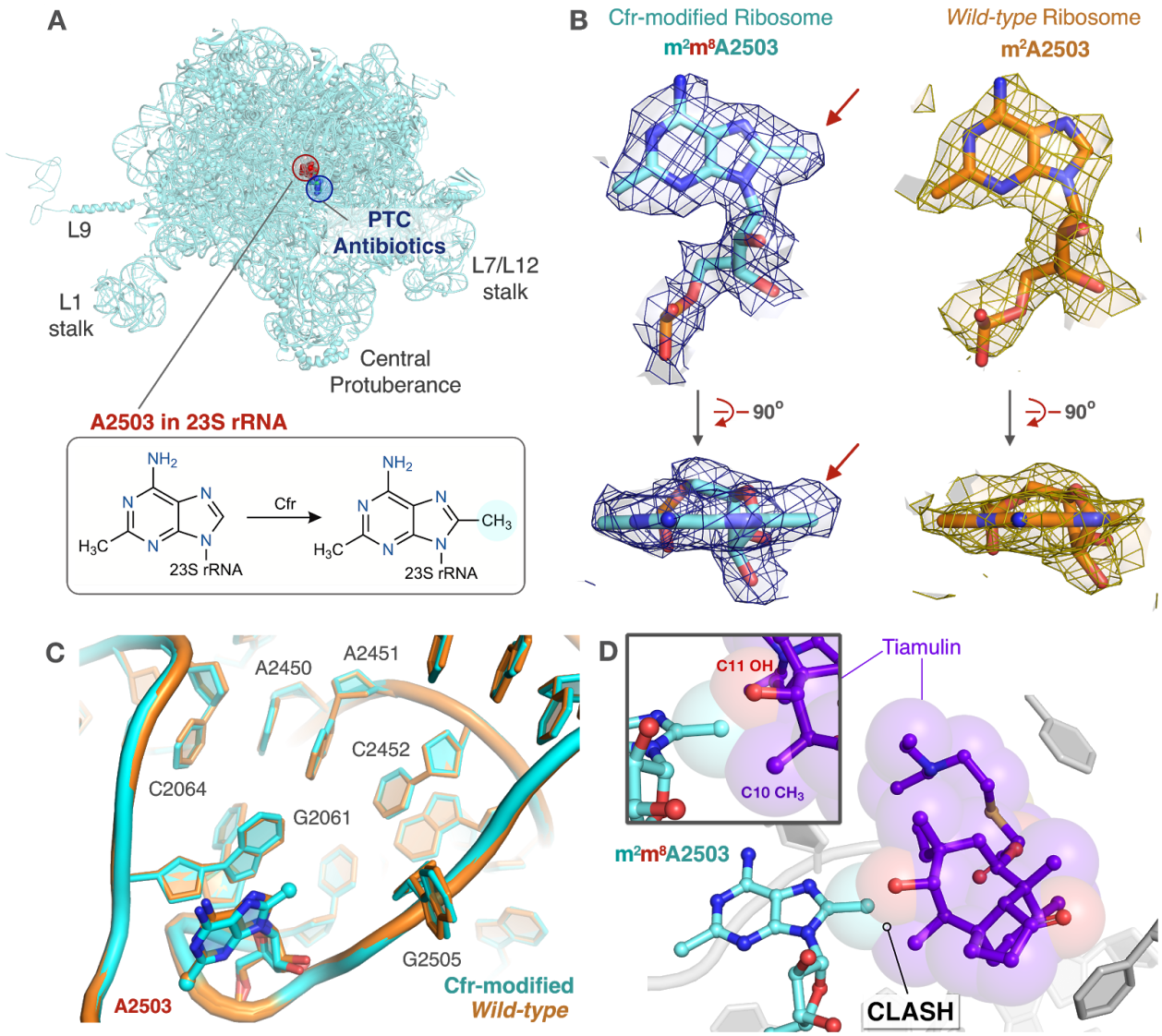

Fig. 5. Near-stoichiometric ribosome methylation by CfrV7 enables structural understanding of Cfr-mediated resistance to antibiotics. (**A**) Cfr-modified 50S ribosomal subunit highlighting adenosine 2503 (A2503) within 23S rRNA and the binding site of PTC-targeting antibiotics. Cfr methylates A2503 at the C8 carbon to produce m^2m^8A2503. (**B**) Cryo-EM density maps of adenosine 2503 in 23S rRNA contoured to 3σ. Cfr-modified (m^2m^8A2503) in cyan. *Wild-type* (m^2A2503) in orange; PDB 6PJ6. (**C**) Close up view of 23S rRNA nucleotides in the 50S ribosomal subunit. Cfr-modified ribosome in cyan. *Wild-type* ribosome in orange; PDB 6PJ6. (**D**) Structural overlay of Cfr-modified ribosome (cyan) and *H. marismortui* 50S ribosome in complex with pleuromutilin antibiotic tiamulin (purple, PDB 3G4S).